Journal of Natural Disaster Science, Volume 25, Number 1, 2003, pp7-15

Near Field Effects of Hidden Seismic Faulting on a Concrete Dam

Tatsuo OHMACHI
Professor, Department of Built Environment, Tokyo Institute of Technology, Yokohama, Japan
Naoyuki KOJIMA
Civil Engineer, Metropolitan Expressway Public Corporation, Tokyo, Japan
(Formerly, Graduate Student, Ditto)
Atsushi MURAKAMI
Engineer, Sumisho Electronics Co. Ltd, Tokyo, Japan
(Formerly, Graduate Student, Ditto)
Nobuhiko KOMABA
Graduate Student, Department of Environmental Science and Technology,
Tokyo Institute of Technology, Yokohama, Japan

(Received 21. Oct., 2002 and in revised form 24 Jun., 2003)

ABSTRACT

The 2000 Western Tottori earthquake (M_J 7.3), Japan, was caused by a hidden seismic fault underlying the Kasho Dam, a 46 m-high concrete gravity dam. Strong-motion accelerometers registered peak accelerations of 2051 at the top of the dam and 531 gal in the lower inspection gallery. Integration of the acceleration records in the gallery showed a permanent displacement of 28 cm to the north, 7 cm to the west, and an uplift of 5 cm. The dam survived the earthquake without serious damage, but the reservoir water level dropped suddenly by 6 cm followed by damped free vibration that continued for several hours. Based on numerical simulation and field observations, the water level change is attributed to ground displacement in the near field and subsequent seiching of the reservoir. The vibration period of the dam in the upstream-downstream direction changed noticeably during the main shock, probably due to hydrodynamic pressure variation. The earthquake caused cracking of concrete floor beams in a sub-gate control room, which was repaired by post-tensioning with steel bars. Micro-tremor measurements were used to evaluate the effectiveness of the repair work.

1. INTRODUCTION

The 2000 Western Tottori earthquake (M_J 7.3), Japan, occurred at 13:30 (local time) on October 6. Kasho Dam, in the near field of this earthquake, is a concrete gravity dam constructed in 1989 with a height of 46.4 m and crest length of 174 m. The seismic design of the dam was basically conducted by the seismic coefficient method using a horizontal coefficient of 0.12. The full water level of the reservoir is EL 118 m, and at the time of the main shock the water level was EL 112 m.

Strong motion accelerometers at the dam registered a peak acceleration of 2051 gal at the top of the dam and 531 gal in the lower inspection gallery (Japan Commission on Large Dams, 2002). Despite such high acceleration, the dam body escaped serious damage, only suffering cracking of the concrete floor in its sub-gate control room. Although no increase in water leakage was recorded, the water level of the reservoir suddenly dropped 6 cm immediately after the main shock. This was followed by damped free vibration that continued for several hours. The drop in reservoir's water level was mysterious and raised concern among dam engineers.

The location of the dam is shown in Fig. 1 together with the hypocenter locations of the main and aftershocks. A seismic fault appears to run through the Kasho Dam site. No clear trace of fault rupturing was found on the ground surface in the epicentral area (Inoue et al., 2002). The earthquake therefore appears to have been caused by seismic rupturing of a hidden fault underlying the dam site (Ohmachi et al., 2002).

2. NEAR-FIELD GROUND DISPLACEMENT

2.1. Ground displacement inferred from strong-motion records

Several monitoring systems are installed at the dam. Three-component strong-motion accelerometers (seismometers) are bolted firmly to the concrete floor of the upper elevator room at EL 124.4 m and on the concrete floor of the lower inspection gallery at EL 87.0 m (Fig. 2). The horizontal components of both accelerometers are set N-S and E-W (the dam axis is oriented N110º E). A reservoir water-level meter is installed in a concrete well on the crest 0.8 m in diameter. Figure 3 presents a downstream view of the dam, showing the elevator tower and small concrete well structure on the downstream side next to the dam's crest.

Acceleration records of the main shock obtained at the two seismometer installations are shown in Fig. 4. Earthquake acceleration was sampled at 100 Hz with 24-bit resolution and reliable from DC to 41 Hz. Seismic ground displacement was estimated by

KEY WORDS: 2000 Western Tottori earthquake, near field, Kasho Dam, strong motion, ground displacement, seiche.

Fig. 1 Map showing locations of the main shock, aftershocks, and Kasho Dam

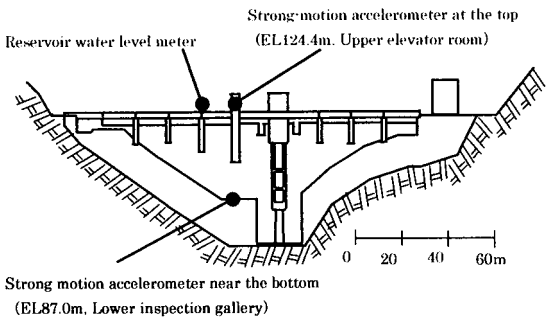

Fig. 2 Locations of strong-motion accelerometers and water level meter at Kasho Dam

Fig. 3 Downstream views of Kasho Dam from the right bank.

twice integrating the acceleration histories at the lower inspection gallery with respect to time.

Figure 5 shows that the dam underwent different modes of displacement in three directions. In the N-S direction, it was displaced linearly to the north with a final permanent displacement of 27.6 cm. In the E-W direction, displacement varied sinusoidally with a final permanent displacement of 6.5 cm to the west. In the vertical direction, displacement showed a sharp upward peak with a final permanent uplift of 4.7 cm.

2.2. Ground displacement from the numerical simulation

Using the fault parameters shown in Table 1 (Geographical

Table 1 Fault parameters used in the simulation

Strike (deg.)	152
Dip (deg.)	86
Rake (deg.)	-7
Dislocation (m)	1.4
Depth of fault (m)	1.0
Fault length (km)	20
Fault width (km)	10

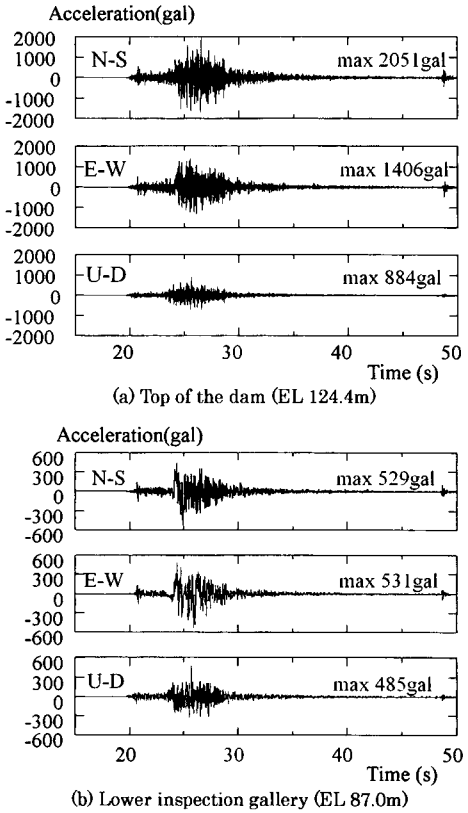

Fig.4 Strong-motion acceleration of the main shock recorded at Kasho Dam.

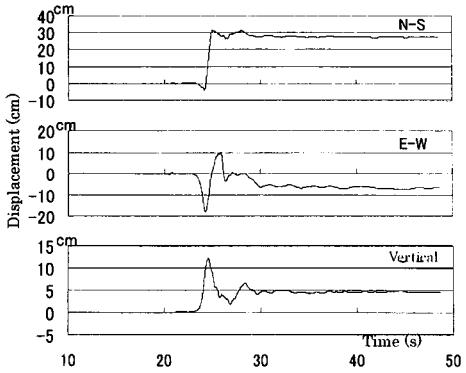

Fig. 5 Displacement histories obtained by integration of acceleration records

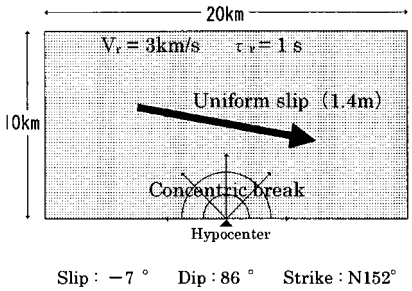

Fig. 6 Seismic fault model for the simulation

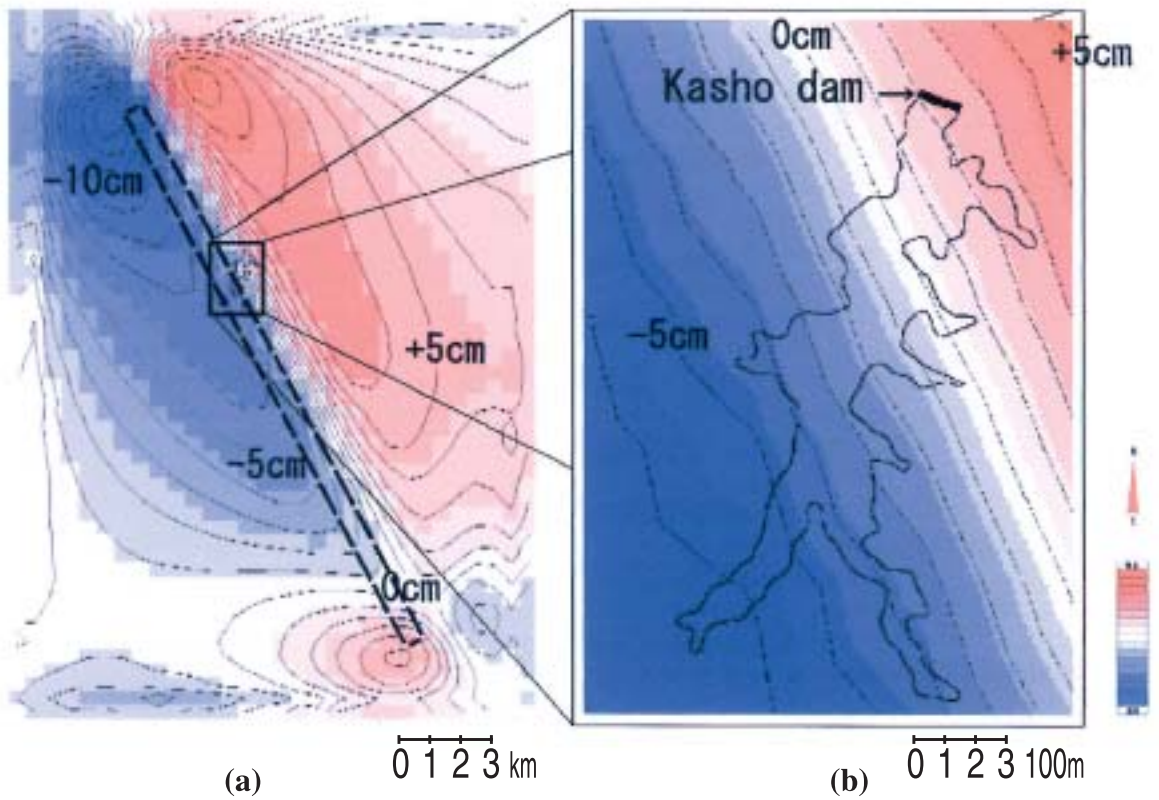

Fig. 7 Vertical ground displacement evaluated from the simulation by (a) BEM and (b) its interpolation (b)

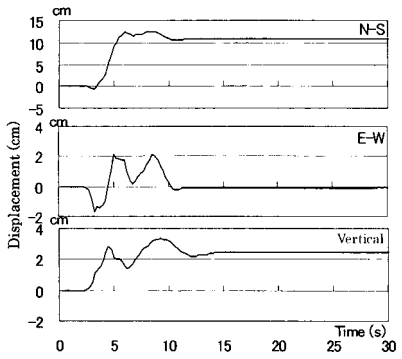

Fig. 8 Ground displacement at Kasho Dam simulated by BEM

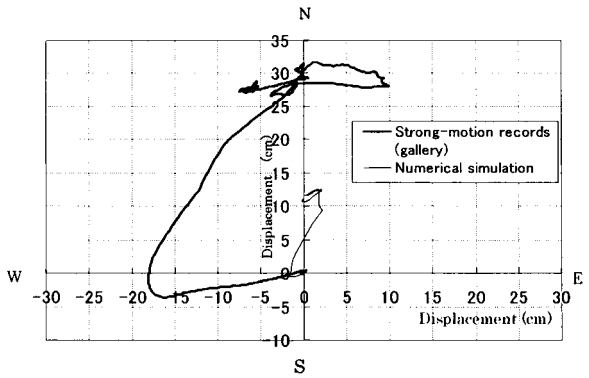

Fig. 9 Horizontal displacement motion trajectories estimated from strong-motion records and the simulation

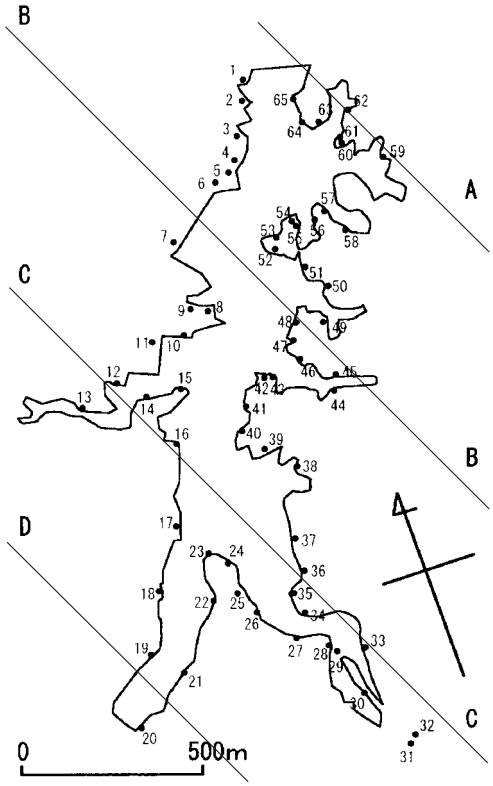

Fig. 10 Observation points along the reservoir for the ground survey

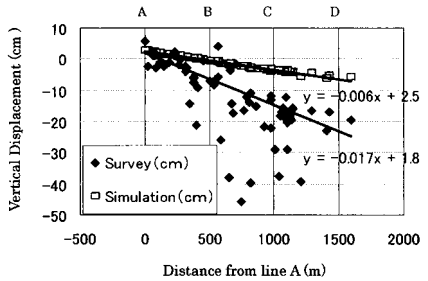

Fig. 11 Comparison of vertical displacements evaluated from the simulation and ground survey

Survey Institute, 2000), the ground displacement associated with the seismic faulting event was simulated by the 3D boundary element method (BEM). The seismic fault of the main shock was a left lateral strike slip fault with a strike of N152° E. Besides the static parameters shown in Table 1, dynamic parameters, e.g., the rupture velocity V_r and rise time τ_r, were tentatively assumed (Fig. 6).

Simulation was conducted on a rectangular area 23 km long (N-S) by 17 km wide (E-W) that encompassed Kasho Dam and its reservoir. The ground was simplified as a half-space of homogenous elasticity with a shear wave velocity of 4 km/s. In the first step of the simulation, seismic ground displacement was calculated at every node of a 500 m×500 m mesh. Results are shown in Fig. 7(a), in which thick broken lines indicate the projection of the fault plane, thick solid lines the reservoir, and thin solid ones lines of equal displacement. The iso-displacement lines run almost parallel to the fault projection in the vicinity of the reservoir, indicating uplift of the reservoir to the northeast and settlement to the southwest.

The displacement in the area indicated by the thick solid lines in Fig. 7(a) was interpolated (Fig. 7(b)). The profile of the reservoir is drawn along the altitude of the design's flood water level (EL123.2 m). Kasho Dam is located at the north end of the reservoir.

Histories of ground displacement around the dam, obtained from interpolation of the simulated displacement, are plotted in Fig. 8. They appear very similar to the recorded displacement histories in Fig. 5, but the amplitudes are somewhat smaller. The simulated permanent ground displacement at the dam is 10.9 cm to the north and 0.1 cm to the west, with an uplift of 2.5 cm. The horizontal displacements shown in Figs. 5 and 8 are plotted in Fig. 9 in terms of motion trajectories. Interestingly, both trajectories in Fig. 9 have features in common; the direction of initial motion, elliptic motion in the final stage, and a large transient shift to the NE or NNE.

2.3. Comparison of vertical displacements found by simulation and a ground survey

After the main shock, a ground survey was conducted at 65 points along the reservoir. Figure 10 shows that the straight lines A to D parallel the fault projection in Fig. 7. With the distance from line A as the reference, the vertical displacements from the simulation and survey are plotted in Fig. 11. Displacements obtained from the survey are almost three times those obtained by simulation, particularly between lines B and C. The differences are attributable to several factors: the inaccuracy of parameters used in the

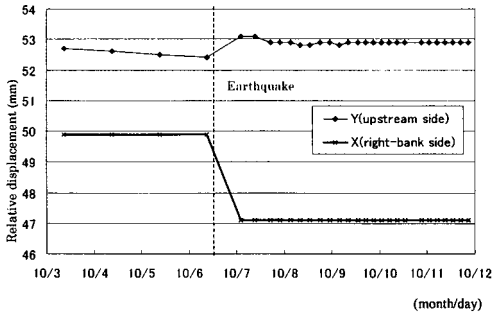

Fig. 12 Relative displacement evaluated from plumb line readings

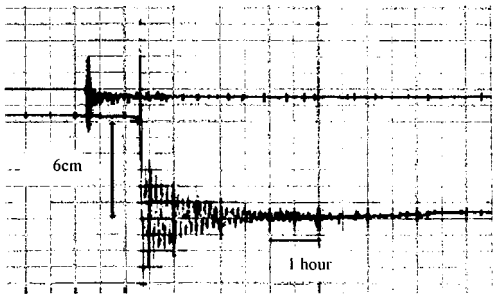

Fig. 13 Records of the reservoir water level at Kasho Dam

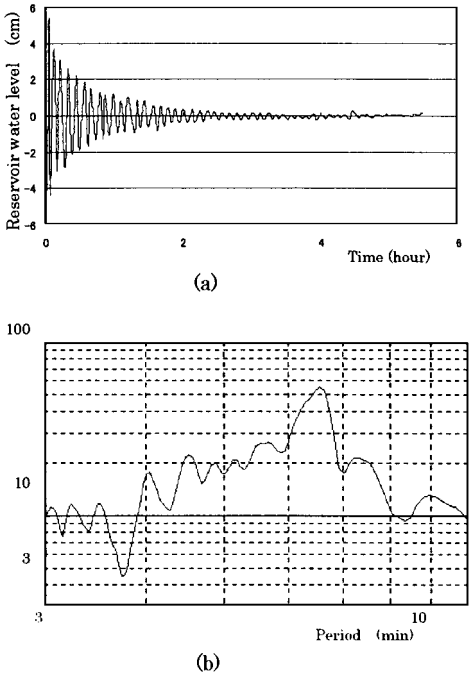

Fig. 14 (a) Reproduced free-vibration history of the water level and (b) the corresponding spectrum

simulation and effects of local site conditions, as well as the effects of the many aftershocks, not considered in the simulation.

2.4. Comparison with plumb line readings

To detect the relative displacement between the top and bottom of the dam, a plumb line was installed in a vertical shaft 30 cm in diameter. The upper end of the steel plumb line is fixed to the floor of the upper elevator room next to the strong motion accelerometer, and the weight on the lower end housed in a measurement device located at EL 89.5 m in the lower inspection gallery. Automatic measurement usually is conducted a few times a day. Readings from the measurements from October 3 to October 13 are plotted in Fig. 12. The main shock induced a relative displacement of –2.8 mm in the x (right bank) direction and 0.7 mm in the y (upstream) direction, with a resultant permanent displacement of 2.9 mm.

If the relative displacement indicated by the plumb line readings is attributable to the inclination of the dam body produced by earthquake-induced ground displacement of its foundation, then the inclination is quantitatively given by the resultant displacement divided by the length of the plumb line; $2.9/34900 = 8.3\times10^{-5}$. In the vicinity of the dam, the inclination of the earthquake-induced ground displacement, as estimated from the simulation, is 6×10^{-5} (Fig. 11). Although this value differs slightly from the inclination determined from plumb line readings in terms of magnitude and direction of inclination, it is reasonable to assume that the dam site was displaced by the seismic faulting of the main shock, as inferred from integration of the strong-motion acceleration.

3. CHANGE IN THE RESERVOIR WATER LEVEL

3.1. Reservoir water level records

The reservoir water level is recorded continuously. The history at the time of the earthquake is shown in Fig. 13. The upper and lower histories in the figure respectively are records with low and high resolutions. They indicate that the water level dropped suddenly by about 6 cm at the time of the main shock, followed by damped free vibration that continued for several hours.

The water level record was reproduced roughly from readings of successive peaks and troughs in the original record. The reproduced history and Fourier spectrum are shown in Fig. 14(a) and (b). The free-vibration characteristics estimated from these findings give a period of 6.5 min and a damping ratio of 2%.

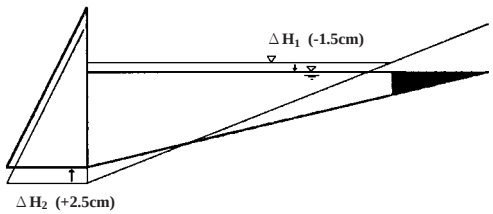

Fig. 15 Schematic explanation of the water level change caused by ground displacement

3.2. Cause of the sudden water level drop

Seismic faulting caused uplifting of the dam body and change in the ground slope of the base of the reservoir as a result of near-field ground displacement. These factors are regarded to constitute the main cause of the sudden drop in the reservoir's water level. A schematic explanation is given in Fig. 15, in which the dam and ground slope before and after the main shock respectively are indicated by thin and thick lines. In the figure, ΔH_1 is the water level change due to the increased reservoir capacity estimated from the average settlement of the reservoir area, and ΔH_2 is the water level change due to the uplifting of the dam. The simulated displace-

ments (Fig. 7) give ΔH_1 of –1.5 cm and ΔH_2 of 2.5 cm, with a corresponding water level change of −4.0 cm ($\Delta H = \Delta H_1 + \Delta H_2$), which is in reasonable agreement with the observed −6.0 cm.

3.3. Seiching of the reservoir

Free vibration of a water body, such as a reservoir, is called seiching (Lamb, 1932). The fundamental period T for a rectangular reservoir is approximated by

$$T = \frac{2a}{\sqrt{gh}} \qquad (1)$$

where a is the length and h the depth of the reservoir, and g the acceleration due to gravity. Introduction of a = 2 km and h = 10 m into Eq. (1) for Kasho Dam gives a period of T = 7.0 min which is fairly close to the observed period of free vibration (6.5 min). Accordingly, the free vibration is thought mainly to be due to the fundamental mode of the seiche. Seiching therefore was simulated by a numerical technique recently developed for tsunami simulation (Ohmachi et al., 2001). This technique essentially involves solving the Navier-Stokes equation for a system by the 3D finite difference method (FDM).

In our simulation, for simplicity the dam and ground were assumed to be rigid. The initial water surface was considered to have the same slope as that obtained from the simulated ground displacement, which was released under the force of gravity, inducing free vibration of the reservoir. The simulated water surface over the entire reservoir for intervals of 50 s from t = 0 to t = 550 s, are shown in Fig. 16. The water level history is shown in Fig. 17, for which the simulated seiche period is 7.5 min (450 s).

In Fig. 16, the reservoir's water surface has a uniform slope at t = 0, the highest water level being at the dam and the lowest at the

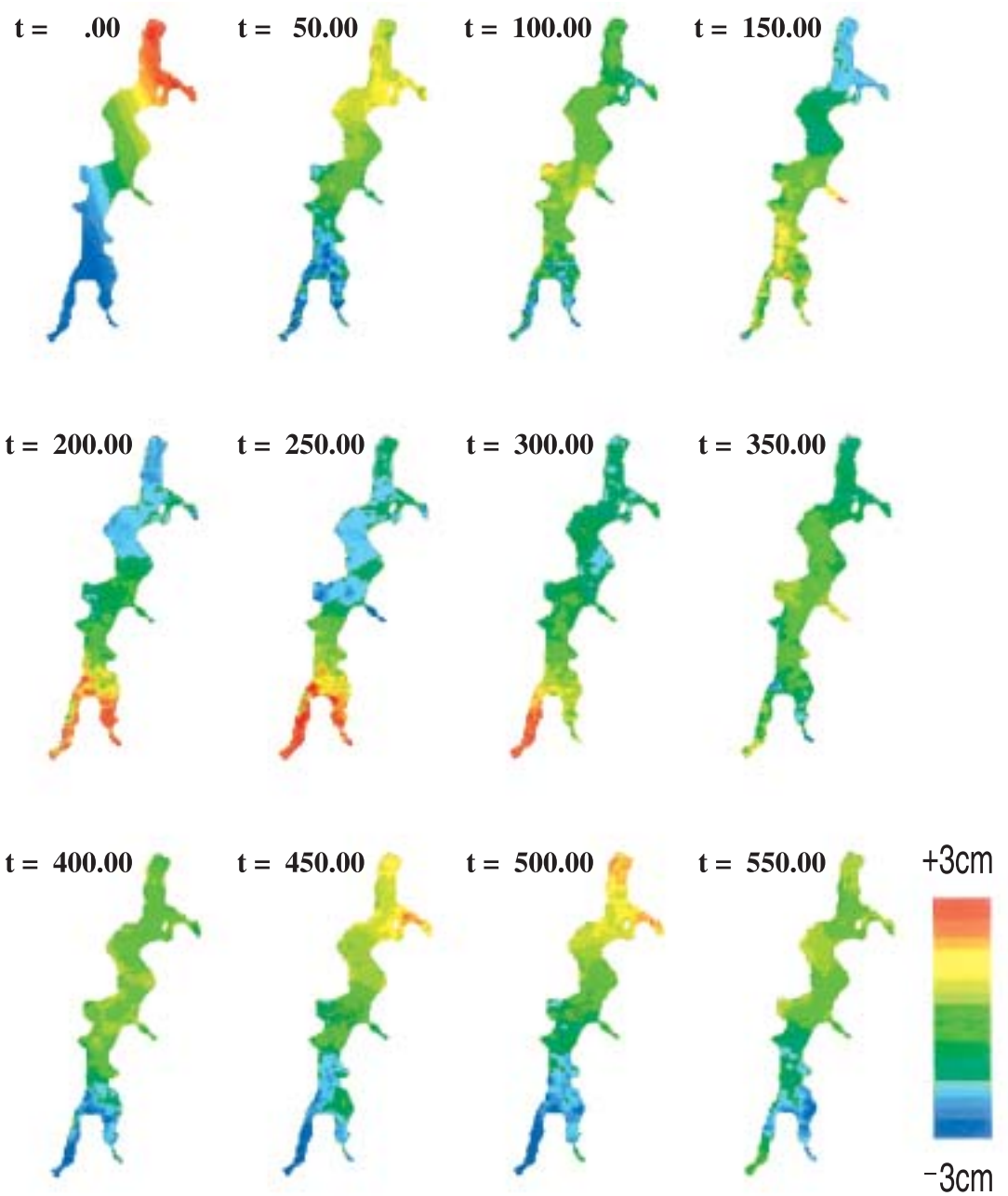

Fig. 16 Water surface of the simulated seiche (time unit : s)

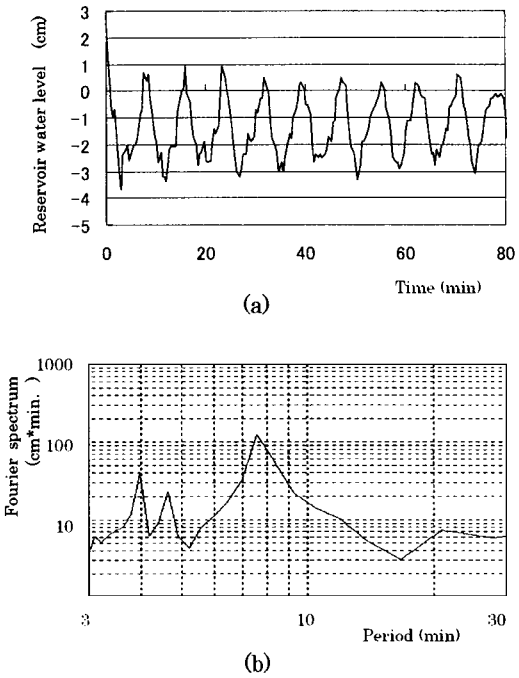

Fig. 17 History of the simulated seiche at Kasho Dam

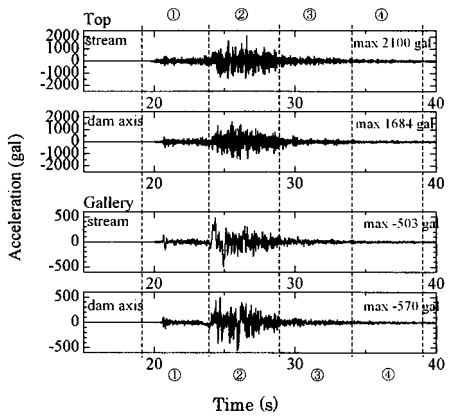

Fig. 18 Horizontal strong-motion records rotated with the azimuth of Kasho Dam

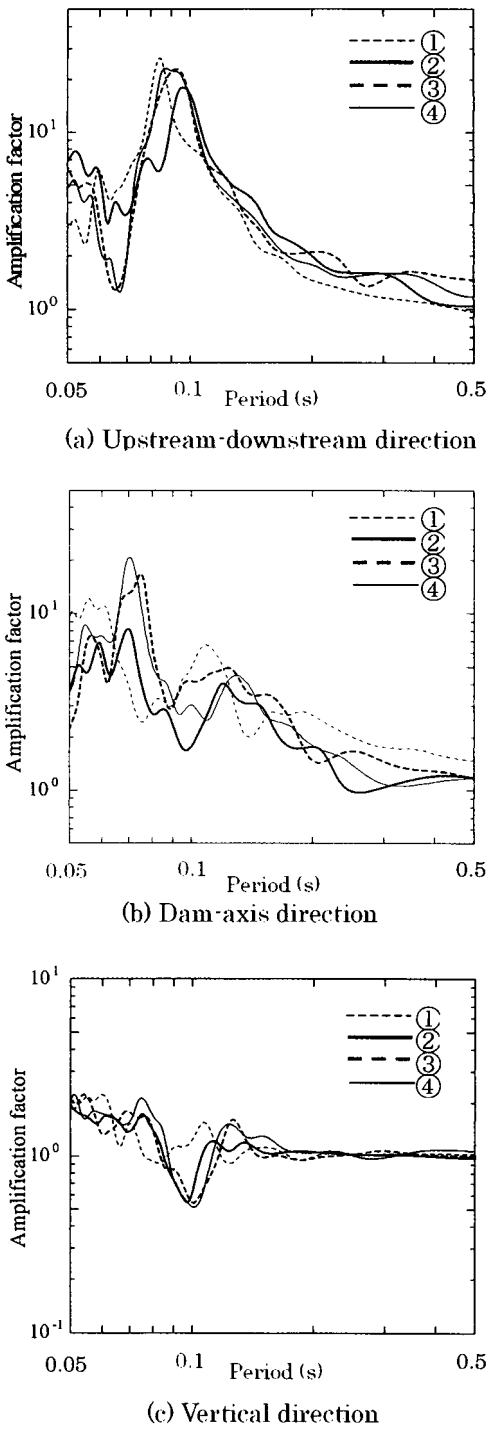

Fig. 19 Amplification factors between the dam top and lower inspection gallery

upstream end. After 200 s, about half of the seiche period, the highest point is at the upstream end and lowest at the dam. After 450 s, the water surface again resembles the initial shape. The water surface pivots on an axis in the middle of the reservoir, indicative that its free vibration motion primarily is due to the fundamental mode of the seiche.

4. STRUCTURAL RESPONSE TO THE EARTHQUAKE AND ITS AFTER EFFECTS

4.1. Change in the vibration period of the dam

Response characteristics of the dam were analyzed by transforming the two horizontal components of the strong-motion records in the N-S and E-W directions, shown in Fig. 4, into the upstream-downstream and dam-axis directions. The transformed acceleration histories are presented in Fig. 18. After transformation, peak accelerations at the top of the dam were 2100 and 1684 gal, respectively in the upstream-downstream and dam-axis directions, and in the lower inspection gallery 570 and 503 gal.

Acceleration histories were divided into four 5.12-s segments (Fig. 18). At the top of the dam, the peak accelerations in the upstream-downstream direction in these segments were 491, 2100, 531 and 227 gal. The amplification factors between the top and lower gallery, calculated from the Fourier spectral ratios between pairs of segments, are shown in Fig. 19. In the upstream-downstream direction, the main peak is about 0.1 s, and appears to be

Table 2 Main and aftershocks recorded at Kasho Dam in the 2000 Western Tottori earthquake

Date and time	M_J	Peak acceleration (gal)		Water level (m)
		Top	Gallery	
10/06 13:30:00	7.3	2100	503	EL112.20
10/07 12:14:10	3.5	332	48	112.18
10/07 18:32:00	3.9	410	73	112.18
10/08 20:51:00	5.3	142	27	112.13
10/09 19:49:40	3.5	212	33	111.95
10/10 02:26:00	3.4	247	36	111.92
10/10 21:57:50	4.4	247	57	111.73
10/12 03:53:20	3.6	52	7	111.33
10/12 08:41:40	3.6	45	6	111.28
10/12 17:07:20	3.5	126	14	111.16
10/13 10:44:10	3.6	91	16	110.93

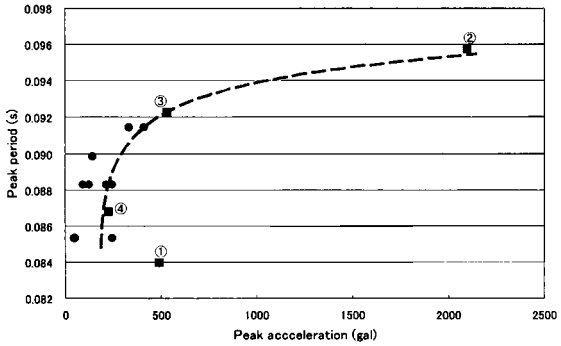

Fig. 20 Peak periods of the dam in the upstream-downstream direction

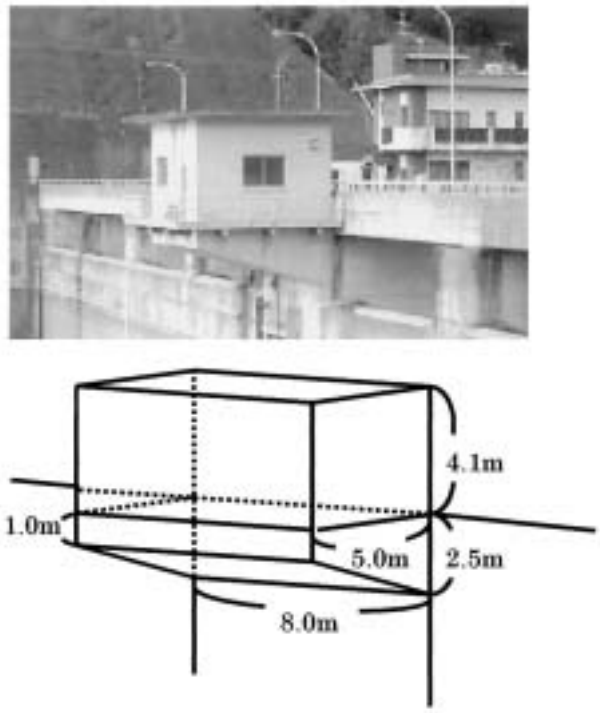

Fig. 21 Sub-gate control room and its dimensions

associated with the fundamental mode of dam vibration. The peak periods of these amplification factors are 0.084, 0.096, 0.092, and 0.087 s for segments 1 through 4. During the main shock, the peak period therefore initially lengthened then shortened, the change

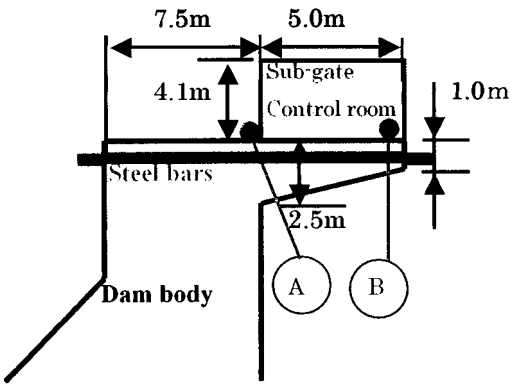

Fig. 22 Schematic explanation showing the post-tensioning of the floor beams and micro-tremor measurement locations

exceeding 10%.

Lengthening of the vibration period during strong earthquake shaking often is due to the non-linearity of material properties. In this case, however, because lengthening is seen only in the upstream-downstream direction, and thereafter the period soon shortened, factors other than the non-linear properties appear to be responsible for the change in the period. One probable factor is the hydrodynamic pressure acting on the upstream face of the dam which would change in proportion to the intensity of earthquake acceleration (Westergaard, 1933).

At Kasho Dam, strong-motion acceleration was well recorded not only during the main shock but the aftershocks (Table 2) (Japan Commission on Large Dams, 2002), which shows peak accelerations in the upstream-downstream direction. Note that in Table 2 the reservoir water at the times of the shocks was almost the same levels, between EL 112.20 and EL 110.93 m. Peak periods in the upstream-downstream direction were similarly obtained from the aftershock acceleration records and plotted against the peak accelerations at the top of the dam (Fig. 20). The peak period tends to increase with the peak acceleration, as shown by the broken line in the figure, whereas the plotted periods are somewhat scattered. Further study is necessary to identify with certainty those factors responsible for the period change.

4.2. Damage and repairs to the sub-gate control room

In the sub-gate control room, concrete was cracked on the floor and sidewalls after the main shock. As shown in Fig. 21, the room is supported by cantilever beams at the center of the dam crest.

The cracks in the cantilever floor-beams were repaired by post-tensioning with steel bars, shown schematically in Fig. 22. Before and after the repairs, micro-tremor measurements were conducted at points on the dam's crest and inside the room. Fourier spectra of the velocity components recorded at Point B, before repair work began, are plotted in Fig. 23(a). The vertical component had the largest amplitude and a peak period at 0.1 s. Spectral ratios of the vertical components between Points A and B are plotted in Fig. 23(b). The peak period apparently was shortened from 0.1 to 0.07 s after the repairs, indicative of a remarkable increase in the rigidity of the cantilever beams as a result of post-tensioning.

In the design of the dam, seismic loading was considered only in the horizontal direction. If the dynamic response characteristics

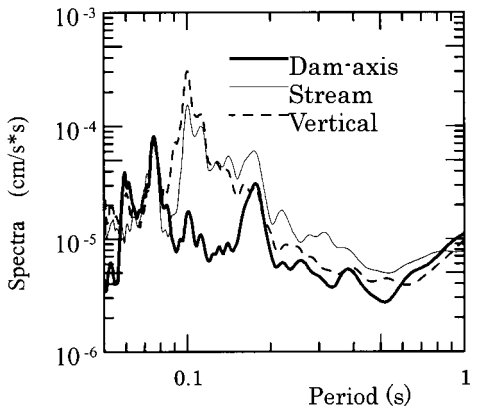

(a) Fourier spectra for beam end (Point B)

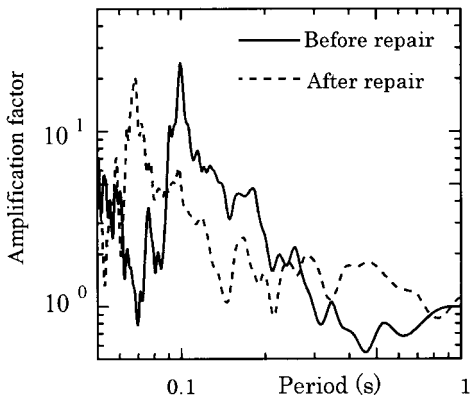

(b) Amplification factors before and after repairs

Fig. 23 Results of micro-tremor measurements.

(or vertical loading) of the sub-gate control room had been taken into account, measures to avoid concrete cracking could have been taken in advance. This cracking in the sub-gate control room during the 2000 earthquake indicates that the earthquake response and/or seismic loading should be considered in seismic designs of not only of dam bodies but of appurtenant structures.

5. CONCLUSIONS

Kasho Dam, a concrete gravity dam, was in the near field of the 2000 Western Tottori earthquake (M_j 7.3) caused by a hidden seismic fault. Strong-motion acceleration at the dam during the main shock exceeded 2000 gal at the top and 500 gal in the lower inspection gallery. Despite these large accelerations, the dam survived the earthquake without serious damage. The reservoir water level, however, dropped markedly immediately after the main shock, and the vibration period of the dam varied by more than 10% during the main shock. The causes and effects of these phenomena were investigated in this study, with the following conclusions:

Seismic rupturing of a hidden fault caused not only dynamic but permanent displacement at the dam site. Integration of the strong-motion acceleration recorded in the lower inspection gallery gave a permanent displacement of 28 cm to the north, 7 cm to the west, and about a 5 cm uplift.

The sudden 6-cm drop in the reservoir water level recorded immediately after the main shock is attributable to permanent displacement of the ground in the near field of the earthquake. The free vibration of the water level after the sudden drop is interpreted as the seiching of reservoir water, characterized by a period of 6.5 min and a damping ratio of 2%.

The plumb line installed at the dam indicated a relative displacement of 2.9 mm between its top and the lower inspection gallery. This displacement is attributable to incremental inclination of the dam's foundation induced by the near-field ground displacement.

During the strong shaking produced by the main shock, the vibration period of the dam body showed a noticeable transient increase in the upstream-downstream direction. There is high probability that the change in period resulted from changes in the hydrodynamic pressure acting on the upstream face of the dam. Further study is required to examine this effect in detail.

The sub-gate control room suffered cracking of its concrete floor beams due to intense shaking during the main shock. The cracks were repaired by post-tensioning with steel bars, resulting in increased beam rigidity. The effectiveness of the repair work was confirmed from micro-tremor measurements. Based on the experiences at this site, it is strongly recommended that the earthquake response not only of the dam body but of appurtenant structures such as sub-gate control rooms be considered in the structural designs of dams.

ACKNOWLEDGMENTS

We thank the Department of Civil Engineering, Tottori Prefecture for providing valuable information regarding the effects of the 2000 earthquake on Kasho Dam. This study was supported in part by the Ministry of Education, Science, Sports and Culture of Japan through Grants-in-Aid for Scientific Research Nos. 13480119 (T. Ohmachi) and 12555134 (K. Kawashima).

REFERENCES

Geographical Survey Institute: http://www.gsi.go.jp/wnew/press-release/2000/1007-2.htm.

Inoue, D., K. Miyakoshi, K. Ueta, A. Miyawaki and K. Matsuura, 2002. Active fault study in the 2000 Tottori-ken seibu earthquake area, Zisin, (Journal of the Seismological Society of Japan), Vol. 5, No.4, 557-573 (in Japanese).

Japan Commission on Large Dams, 2002. Acceleration records on dams and foundations No. 2 (CD-ROM version).

Lamb, H. 1932. Hydrodynamics, Cambridge Univ. Press, Cambridge, U. K. 190-191.

Ohmachi, T., N. Kojima and A. Murakami, 2002. Ground displacement and change in reservoir water level due to seismic rupturing of a hidden fault underlying a dam site, Jour. Str. Mech. Earthquake Eng., JSCE, No.710/I-60, 337-346 (in Japanese).

Ohmachi, T., H. Tsukiyama and H. Matsumoto, 2001. Simulation of tsunami induced by dynamic displacement of seabed due to seismic faulting, Bull. Seism. Soc. Am., Vol. 91, No.6, 1898-1909.

Westergaard, H. M., 1933. Water pressure on dams during earthquakes, Trans. ASCE 95, 418-433.